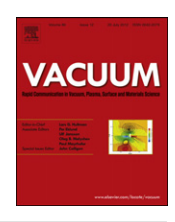


#### Contents lists available at SciVerse ScienceDirect

## Vacuum

journal homepage: www.elsevier.com/locate/vacuum



## Rapid communication

# Effect of Si content on the microstructure and mechanical properties of Mo–Al–Si–N coatings

J.F. Yang a,\*, B. Prakash b, Y. Jiang A, X.P. Wang A, Q.F. Fang B

<sup>a</sup> Key Laboratory of Materials Physics, Institute of Solid State Physics, Chinese Academy of Sciences, 350 KeXueYuan Road, PO Box 1129, Hefei 230031, People's Republic of China <sup>b</sup> Department of Applied Physics and Mechanical Engineering, Lulea University of Technology, SE-971 87 Luleå, Sweden

#### ARTICLE INFO

Article history: Received 3 May 2012 Received in revised form 9 May 2012 Accepted 9 May 2012

Keywords: Nanocomposite coatings Magnetron sputtering Mo-Al-Si-N Hardness

#### ABSTRACT

Mo–Al (Al/(Mo + Al) = 6.5%)–Si–N coatings with silicon content ranging from 0 to 17 at.% were fabricated using d.c. reactive unbalanced magnetron sputtering technique in an Ar–N<sub>2</sub> mixture. Surface morphology, element and phase composition, residual stress and nanohardness of these coatings were studied by scanned electrical microscopy (SEM), X-ray photoelectron spectroscopy (XPS), X-ray diffraction (XRD), residual stress tester, and nanoindenter, respectively.

Results exhibit that the residual stress built in the coating is compressive in nature ranging between 0.6 and 1.8 GPa. Nanohardness of Mo–Al–Si–N coatings increased at first and then decreased with silicon content, reaching a maximum value of 36 GPa at 8.3 at.% Si. The optimum hardness could be ascribed to higher compressive stress and nanocomposite structure where nanocrystallite Mo–Al–Si–N embedded in amorphous  $Si_3N_4$  matrix.

© 2012 Elsevier Ltd. All rights reserved.

Over the last decades, coatings of transition metal nitrides and carbides have been widely used as protective coatings for drilling, machining and cutting tools. Among nitride coatings, Ti–Al–N coatings dominated the industrial applications for dry machining due to their high temperature oxidation resistance and agehardening abilities [1–3]. However, the fast development in high speeds and dry cutting application demands constant improvement in hardness and oxidation resistance temperature of Ti–Al–N coatings. In recent years, a lot of effort was done by alloying Ti–Al–N based coatings with several elements acting in different ways [4–6]. It was found that quaternary Ti–Al–Si–N coatings can provide better mechanical properties than that of ternary Ti–Al–N coatings, where Si existed either in the form of amorphous nitride or as an interstitial solid solution with Si atoms dissolving into Ti–Al–N crystal lattice [7,8].

In contrast to Ti–N based coatings, Mo–N coatings exhibited lower friction coefficient due to the formation of a self-lubricating layer of MoO<sub>3</sub> [9], better adhesion with steel substrate owing to the good solubility of molybdenum in iron based materials [10], lower hardness and lower oxidation resistant temperature between 350 and 400 °C [11]. The addition of third element into Mo–N coatings can improve the hardness and oxidation resistance

properties of Mo–N coatings. It was found that the hardness of Mo–N films could increase to 29 GPa by addition of Al into Mo–N coating [12], even up to 47 GPa by incorporation of W into Mo–N films [13], the oxidation resistant temperature could increase to 700 °C for Mo–Al–N coating [12], even exceed 1000 °C for Mo–Si–N coating with high content of Si [14]. However, the improvement of one property is usually at the cost of other properties.

In our work, by analogy with Ti–Al–Si–N coating system, Al and Si were incorporated into Mo–N coating simultaneously using d.c. magnetron sputtering technique in order to obtain improved comprehensive properties by the synergetic effect of Mo–Al–N and Mo–Si–N coatings, and the effect of Si content on the microstructure, hardness, residual stress of Mo–Al–Si–N coatings was investigated in details.

Mo—Al—Si—N coatings with various silicon contents were synthesized by dc reactive magnetron sputtering technique from a Mo target embedded with Si and Al pellets. The Si concentration in the coatings can be easily controlled by changing the number of silicon pellets.

Silicon wafers were used as substrates. Before deposition, all substrates were ultrasonically cleaned in a bath of acetone for 5 min, ethanol for 10 min, and de-ionized water for 10 min successively, and then dried with dry  $N_2$ . After cleaning, the substrates were immediately mounted on the substrate holder. The substrate-to-target distance was 60 mm.

<sup>\*</sup> Corresponding author. Tel.: +86 551 5591439x207; fax: +86 551 5591434. E-mail address: jfyang@issp.ac.cn (J.F. Yang).

The vacuum chamber was then evacuated to a base pressure of  $1.5\times 10^{-3}$  Pa, followed by heating the substrate up to a temperature of 450 °C. Before coating deposition, the target was pre-sputtered for 20 min at an argon pressure of 2 Pa and direct current (dc) power of 120 W. Thereafter, the sputter process was initiated by introducing  $N_2$  gas into vacuum chamber, and maintaining the work pressure and sputtering power at 0.5 Pa and 100 W, respectively. During sputtering process, bias voltage of about -50~V was applied to the substrate, the mass flow rate of Ar gas and nitrogen gas were fixed at 40 and 30 sccm, respectively.

Surface morphology of coatings was observed with field-emission scanning electron microscope (FESEM, Sirion 200, FEI). Thickness of Mo–Al–Si–N coatings is about 2.5–3  $\mu m$  as determined by cross-section SEM. Grazing incidence X-ray diffraction (Philips X'pert PRO MPD) with incidence angle of 1° using monochromatized Cu K $\alpha$  radiation was adopted to identify the crystal structure of the coatings. Lattice constant was evaluated by the whole pattern refinement of the XRD patterns using the fullprof program. Average grain size of Mo–Al–Si–N coatings was estimated using Williamson–Hall equation [15],

$$\frac{B\cos\theta}{\lambda} = \frac{0.9}{C} + \frac{4\varepsilon\sin\theta}{\lambda}$$

where B is the full width at half maximum (FWHM) experimentally obtained for a Bragg angle  $\theta$ ,  $\lambda$  is the wavelength of the Cu Ka radiation. C is the crystallite size, and  $\varepsilon$  is the approximate upper limit of the strain. By plotting  $(B\cos\theta)/\lambda$  versus  $(4\sin\theta)/\lambda$ , i.e. Williamson—Hall plot, crystallite size could be obtained from the intercept (0.9/c), and was listed in Table 1.

An X-ray photoelectron spectroscopy (XPS, Japan, Axis ultra DLD) with Al (mono)  $K\alpha$  irradiation at a pass energy of 160 eV was used to characterize the chemical bonds of the deposited coatings. Before commencing the measurement, Ar+ ion beam with an energy of 3 keV was used to etch the sample surface for 30 min to remove contaminants. The relative atomic ratios of the elements were calculated from the areas under their XPS peaks by considering the relative sensitivity factors based on Wagner data analysis system [16], as exhibited in Table 1. The binding energies were referenced to the C 1s line at 284.6 eV [17]. Microstructural information on the coatings was obtained by a field emission transmission electron microscope (JEOL, JEM-2010) operating at 200 kV.

Hardness of the films was measured with a nanoindentation apparatus (MTS NANO Indenter® G200) at room temperature. The data of hardness was averaged from 9 indentation tests for each sample to improve measurement accuracy, and the measurements were calibrated with reference sample of fused quartz (hardness of 10 GPa). The residual stress was examined using a residual stress tester [J&L Tech. JLCST022] by which the change of radius of

**Table 1**Elemental composition and average grain size of Mo–Al–Si–N coatings determined by XPS and Williamson–Hall equation, respectively.

Coating number	Elemental composition (at.%)				Average grain
	Si	Al	Мо	N	size (nm)
a	0.0	4.0	57.5	38.5	40
b	1.1	3.9	55.4	39.6	37
c	2.0	3.8	53.9	40.3	35
d	2.8	3.6	52.5	41.1	31
e	3.7	3.5	49.9	42.9	25
f	4.5	3.3	48.2	44.0	20
g	5.2	3.2	46.2	45.4	16
h	8.3	2.9	41.2	47.6	9
i	13.0	2.4	33.9	50.7	
j	17.0	1.9	26.7	54.4	

curvature of silicon substrate before and after coating deposition was first measured using laser beam, and then residual stress was determined based on Stoney's equation.

Fig. 1 shows the X-ray diffraction (XRD) pattern of as deposited Mo-Al-N and Mo-Al-Si-N coatings with different silicon content. The diffraction pattern of Mo-Al-N coating exhibited five diffraction peaks centering at approximately 37°, 43°, 63°, 75°, 79°, corresponding to the Bragg diffraction lines from the (111), (200). (220), (311) and (222) planes of face-centered-cubic Mo-Al-N phase where some Mo atoms in fcc γ-Mo<sub>2</sub>N crystal lattice were replaced by Al atoms [12]. As silicon was introduced into the Mo-Al-N coating, the diffraction peak intensities of Mo-Al-Si-N coatings decreased gradually, and became X-ray amorphous at and above 13 at.% Si. In addition, it can be observed that with silicon content increasing, the diffraction peak of Mo-Al-Si-N coatings shifted to lower diffraction angle due to the increase in lattice constant from 4.171 to 4.182, 4.195, 4.210, 4.223, 4.230, and 4.242 Å as silicon content in Mo-Al-Si-N coatings increase from 0 at.% to 1.1 at.%, 2 at.%, 2.8 at.%, 3.7 at.%, 4.5 at.%, and 5.2 at.%, respectively. The increase of lattice constant with silicon concentration was ascribed to that some silicon atoms dissolved into interstitial sites in Mo-Al-N crystal lattice. In contrast to lattice constant, With the increase of Si content from 0 to 8.3 at.% the crystallite size of Mo-Al-Si-N coatings decreased gradually from about 40 nm to 9 nm. The same phenomena have already been reported in Ti-Al-Si-N [18] and Cr-Mo-Si-N [19] systems. No X-ray diffraction peaks from crystalline Si<sub>3</sub>N<sub>4</sub>, MoSi<sub>2</sub> and Mo<sub>3</sub>Si<sub>5</sub> were detected. Moreover, it can be seen that Mo-Al-N coatings have a very strong (200) preferential orientation. As the silicon content is between 1.1 at.% and 3.7 at.%, a mixed texture of (200) and (220) occurs, and then changed to (220) with further increase of silicon content. Development of preferential orientation in non-epitaxial thin films is primarily governed by minimization of the sum of surface energy and strain energy under the restrictions imposed by kinetics [20]. The occurrence of (200) preferential orientation in Mo-Al-N coating is due to (200) plane possessing lowest surface energy in face centered cubic structure, which could be understand from the thermodynamics point of view. Similar result was reported in fcc Ti-N coatings [21]. The occurrence of (220) preferential orientation in Mo-Al-Si-N coatings is still not fully understood. It is known that atomic planar density of (100), (110), (111) plane in

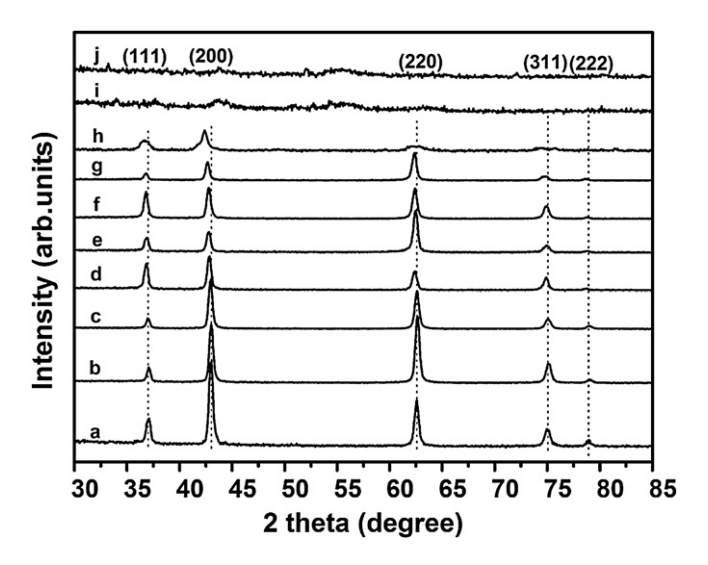


**Fig. 1.** XRD patterns of Mo–Al–Si–N coatings deposited with different Si content: (a) 0 at.% Si, (b) 1.1 at.% Si, (c) 2 at.% Si, (d) 2.8 at.% Si, (e) 3.7 at.% Si, (f) 4.5 at.% Si, (g) 5.2 at.% Si, (h) 8.3 at.% Si, (i) 13 at.% Si, (j) 17 at.% Si.

# Download English Version:

# https://daneshyari.com/en/article/1688888

Download Persian Version:

https://daneshyari.com/article/1688888

**Daneshyari.com**